Insights into Surface Recombination of Polycrystalline Perovskite Films via Injection-Dependent Lifetime Analysis

Robert (μRob) Lee-Chin[1*], Arman Mahboubi Soufiani[1*], Jianghui Zhang[1], Germain Rey[1], Anita Ho-Baillie[1,2], Peter Reece[3], Thorsten Trupke[1], and Ziv Hameiri[1]
[1]School of Photovoltaic and Renewable Energy Engineering, University of New South Wales, Sydney, Australia
[2]School of Physics and the University of Sydney Nano Institute, University of Sydney, Sydney, Australia
[3]School of Physics, University of New South Wales, Sydney, Australia

Lead-halide based perovskite semiconductors exhibit long effective minority carrier lifetimes (τ_{eff}) approaching the radiative limit [1]. However, further improvements remain bottlenecked by non-radiative interfacial recombination which varies with the excess carrier densities (Δn). It is therefore crucial to establish methods which allow quantitative identification of the contribution of surfaces and interfaces to the perovskite-based devices' recombination losses [2].

Owing to the large radiative recombination coefficient (B_{rad}) of perovskites, photoluminescence (PL)-based techniques such as time-resolved PL (TR-PL) [3] and absolute steady-state spectral PL (SS-PL) [4] have been used to identify the impact of different interfaces (passivation layer or selective contacts) on the device recombination. These techniques measure the total device recombination of the bulk and *all* interfaces, therefore requiring assumptions and/or analysis methods to decouple the surface recombination contribution. Approaches to extract the interfacial recombination parameters include fitting of TR-PL with rate equations, correlating the ideality factors (n_{id}) from light-intensity (Φ) dependent SS-PL with the quasi-Fermi level splitting ($\Delta\mu$) [5] or full-device open-circuit voltages (V_{OC}) or through device simulations to match the measured TR-PL and SS-PL/$\Delta\mu$ [6]. However, such methods may lead to contradictory interpretations, for example, recently it was reported that when the device V_{OC} is interface-limited, the extracted n_{id} from a linear fit to the Suns-V_{OC} semi-logarithmic plots approaches one, whereas under bulk limiting condition the n_{id} gets closer to two [5]. However, these interpretations are in contradiction with other studies in which reducing the surface/interface recombination was argued to reduce n_{id} [7, 8].

In this study, we propose quantifying the surface recombination based on analysing the *injection-dependent effective lifetime* [$\tau_{eff}(\Delta n)$] determined from the absolute SS-PL. Some of the advantages of this approach include:

1. $\tau_{eff}(\Delta n)$ curves are less subject to incorrect interpretation compared to correlations of n_{id} with the V_{OC}/$\Delta\mu$. This is because $\tau_{eff}(\Delta n)$ is a direct measure of the injection-dependent recombination and is directly related to the device recombination parameters.
2. The injection-dependent B_{rad} is experimentally determined. This is important as radiative recombination in perovskites contributes significantly to the total device recombination and is sample-dependent [9]. In addition, there has been speculations of a non-radiative bi-molecular recombination coefficient ($B_{non\text{-}rad}$) [10], which can be explored through the access to $\tau_{eff}(\Delta n)$.
3. $\tau_{eff}(\Delta n)$ measured with varying film thicknesses (W) allows the injection-dependent bulk and surface contributions to be separated [11].

Here, we measured $\tau_{eff}(\Delta n)$ curves for various high-quality $Cs_{0.05}FA_{0.79}MA_{0.16}Pb(I_{0.83}Br_{0.17})_3$ films (W of ~480 nm) deposited on glass:

1. Untreated perovskite film (Bare)
2. Passivated film with tri-n-octylphosphine oxide (TOPO)
3. Selective contact, poly(triarylamine) (PTAA), on perovskite film

In Figure 1A, examples of the PL spectra of the three samples, measured at 1-Sun equivalent photon flux, are presented. The Δμ values are in good-agreement with the literature [12]. Figure 1B shows the corresponding $\tau_{eff}(\Delta n)$ curves. Note that based on recent Hall-effect [13] and ultraviolet photoelectron spectroscopy studies [14], the bulk dopant density (N_{dop}) in the perovskite composition studied here is safely considered to be $<10^{12}$ cm^{-3}. Therefore, the $\tau_{eff}(\Delta n)$ curves are representative of the recombination in the high-injection regime. We observe that at $\Delta n<10^{15}$ cm^{-3} τ_{eff} is increasing from PTAA to Bare to TOPO. This behaviour is consistent with recombination at the perovskite/air or perovskite/contact interface decreasing, respectively. However, τ_{eff} at $\Delta n>5\times10^{15}$ cm^{-3} demonstrates an injection-dependence following the radiative lifetime (τ_{rad}). We quantify this behaviour using the surface recombination parameter (J_{0s}) [15], which parameterises the recombination arising from band-bending at interfaces and is valid in high-injection. Note that the intrinsic carrier density (n_i) needed to determine J_{0s} is calculated using the band-gap energy (E_g) obtained from the measured spectral PL and the reported effective masses from magneto-optical experiments [16].

J_{0s} was determined for the three samples as can be seen in Figure 1C. J_{0s} of the TOPO-passivated sample is a third of the J_{0s} of the untreated bare film and the perovskite film contacted with PTAA. Previous microscopic-PL studies have shown that TOPO provides excellent passivation for both the surfaces and the grain boundaries [17], which agrees well with our observation of overall higher τ_{eff} compared to the non-TOPO samples. We thus, tentatively suggest that the determined J_{0s} can be attributed to recombination at the grain boundaries, passivated in the TOPO case, while remained almost untouched in the bare film and PTAA-contacted film. Note that the glass-side can be assumed to be relatively recombination inert based on studies in which surface passivation using TOPO at the air-interface produced τ_{eff} close to the radiative-limit of the corresponding perovskite film [17].

In summary, we analysed the injection-dependent effective lifetime of few different perovskite film stacks. The intrinsic bulk recombination lifetime of relevance, here radiative recombination, is removed for subsequent defect-mediated loss analysis. Our initial results suggest that J_{0s} may be used to quantify the recombination at grain boundaries. Parameterisation of the injection-dependence at $\Delta n<10^{15}$ cm^{-3} requires further in-depth examination, currently under investigation.

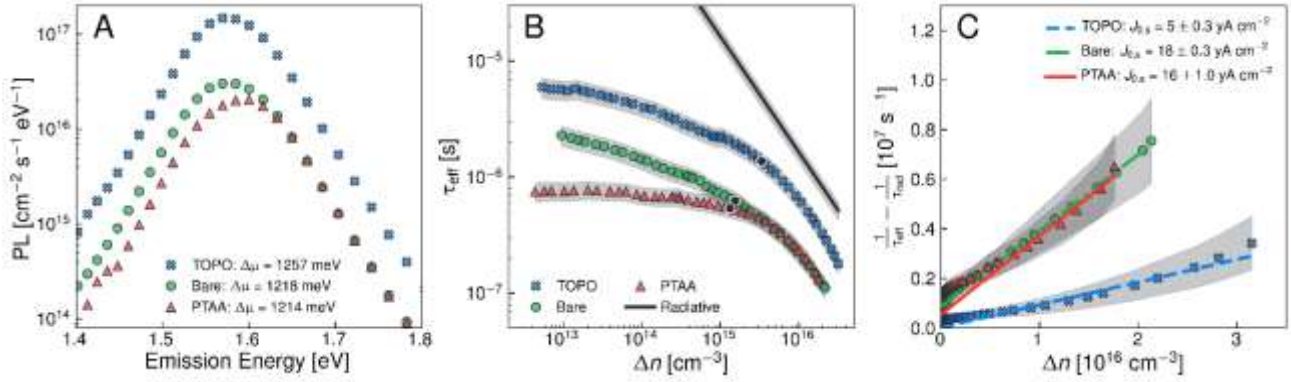

Figure **1**. Panel A illustrates the PL spectra at absorbed photon flux of 1-Sun equivalent. Panel B provides the corresponding $\tau_{eff}(\Delta n)$ curves. The black symbol on each curve is the 1-Sun equivalent excess carrier density. The radiative lifetime, corrected for photon recycling [3], is shown for comparison. The filled-in areas represent the experimental uncertainties of τ_{eff} and Δn (Δμ). Panel C presents the Kane-Swanson method [11] applied to extract J_{0s}. The filled-in areas represent the experimental uncertainties of τ_{eff} and τ_{rad}. Please note that: 1 yA = 10^{-24} A.

References

1. Braly, I.L., et al., Hybrid perovskite films approaching the radiative limit with over 90% photoluminescence quantum efficiency. Nature Photonics, 2018. **12**(6): p. 355-361.
2. Soufiani, A.M., et al., Lessons Learnt from Spatially Resolved Electro- and Photoluminescence Imaging: Interfacial Delamination in CH3NH3PbI3 Planar Perovskite Solar Cells upon Illumination. Adv. Energy Mater., 2016. **7**: p. 1602111.
3. Staub, F., et al., Beyond Bulk Lifetimes: Insights into Lead Halide Perovskite Films from Time-Resolved Photoluminescence. Physical Review Applied, 2016. **6**(4): p. 044017.
4. Kirchartz, T., et al., Photoluminescence-Based Characterization of Halide Perovskites for Photovoltaics. Advanced Energy Materials. **10**(26): p. 1904134.
5. Caprioglio, P., et al., On the Origin of the Ideality Factor in Perovskite Solar Cells. Advanced Energy Materials, 2020: p. 2000502.
6. Haddad, J., et al., Analyzing Interface Recombination in Lead-Halide Perovskite Solar Cells with Organic and Inorganic Hole-Transport Layers. Advanced Materials Interfaces, 2020: p. 2000366.
7. Jiang, Q., et al., Surface passivation of perovskite film for efficient solar cells. Nature Photonics, 2019. **13**(7): p. 460-466.
8. Sherkar, T.S., et al., Recombination in Perovskite Solar Cells: Significance of Grain Boundaries, Interface Traps, and Defect Ions. ACS Energy Letters, 2017. **2**(5): p. 1214-1222.
9. Staub, F., et al., Manipulating the Net Radiative Recombination Rate in Lead Halide Perovskite Films by Modification of Light Outcoupling. The Journal of Physical Chemistry Letters, 2017. **8**(20): p. 5084-5090.
10. deQuilettes, D.W., et al., Charge-Carrier Recombination in Halide Perovskites. Chemical Reviews, 2019. **119**(20): p. 11007-11019.
11. Kane, D.E. and R.M. Swanson. Measurement of the Emitter Saturation Current by a Contactless Photoconductivity Decay Method. in IEEE PV Specialist Conference. 1985. p. 578-583.
12. Stolterfoht, M., et al., The impact of energy alignment and interfacial recombination on the internal and external open-circuit voltage of perovskite solar cells. Energy & Environmental Science, 2019. **12**(9): p. 2778-2788.
13. Gunawan, O., et al., Carrier-resolved photo-Hall effect. Nature, 2019. **575**(7781): p. 151-155.
14. Yang, J.-P., et al., Band Dispersion and Hole Effective Mass of Methylammonium Lead Iodide Perovskite. Solar RRL, 2018. **2**(10): p. 1800132.
15. McIntosh, K.R. and L.E. Black, On effective surface recombination parameters. Journal of Applied Physics, 2014. **116**(1): p. 014503.
16. Mahboubi Soufiani, A., et al., Impact of microstructure on the electron-hole interaction in lead halide perovskites. Energy & Environmental Science, 2017. **10**: p. 1358-1366.
17. deQuilettes, D.W., et al., Photoluminescence Lifetimes Exceeding 8 μs and Quantum Yields Exceeding 30% in Hybrid Perovskite Thin Films by Ligand Passivation. ACS Energy Letters, 2016. **1**(2): p. 438-444.